

JGR Atmospheres

RESEARCH ARTICLE

10.1029/2020JD033369

Special Section:

Atmospheric PM_{2.5} in China: physics, chemistry, measurements, and modeling

Key Points:

- The secondary inorganic aerosols were mainly originated from photochemical generations during winter in Lanzhou
- The contributions of both inorganic and organic secondary species decreased with increasing particulate pollution
- The influence of vehicle exhaust emissions on particulate pollution increased with increasing particulate pollution

Supporting Information:

- Supporting Information S1

Correspondence to:

P. Tian,
tianpf@lzu.edu.cn

Citation:

Du, T., Wang, M., Guan, X., Zhang, M., Zeng, H., Chang, Y., et al. (2020). Characteristics and formation mechanisms of winter particulate pollution in Lanzhou, Northwest China. *Journal of Geophysical Research: Atmospheres*, 125, e2020JD033369. <https://doi.org/10.1029/2020JD033369>

Received 24 JUN 2020

Accepted 30 JUL 2020

Accepted article online 26 AUG 2020

Author Contributions:

Conceptualization: Pengfei Tian

Data curation: Tao Du, Huiyu Zeng, Yi Chang, Jinsen Shi

Formal analysis: Tao Du, Min Wang, Xu Guan, Min Zhang, Pengfei Tian

Funding acquisition: Lei Zhang, Pengfei Tian

Methodology: Tao Du



Supervision: Lei Zhang

Validation: Tao Du, Min Wang, Xu Guan, Min Zhang, Pengfei Tian

Visualization: Tao Du, Min Wang, Xu Guan, Min Zhang, Huiyu Zeng, Pengfei Tian, Chenguang Tang
(continued)

©2020. American Geophysical Union.
All Rights Reserved.

Characteristics and Formation Mechanisms of Winter Particulate Pollution in Lanzhou, Northwest China

Tao Du^{1,2}, Min Wang^{1,2}, Xu Guan^{1,2}, Min Zhang^{1,2}, Huiyu Zeng^{1,2}, Yi Chang³, Lei Zhang^{1,2} , Pengfei Tian^{1,2} , Jinsen Shi^{1,2}, and Chenguang Tang^{1,2}

¹Key Laboratory for Semi-Arid Climate Change of the Ministry of Education, College of Atmospheric Sciences, Lanzhou University, Lanzhou, China, ²Collaborative Innovation Center for Western Ecological Safety, Lanzhou University, Lanzhou, China, ³Gansu Province Environmental Monitoring Center, Lanzhou, China

Abstract The formation mechanisms of particulate pollution in Lanzhou, which used to be one of the most polluted cities across the world, remain unclear even though air pollution in Lanzhou has been improved in recent decades. Multiple online data during 2019–2020 winter was used to analyze the characteristics and reveal the formation mechanisms of particulate pollution in Lanzhou. Organic matter, nitrate, sulfate, and ammonium accounted for 35.8%, 16.6%, 12.7%, and 10.8%, respectively, of PM_{2.5} mass. The contribution of secondary inorganic aerosols decreased from low to high particulate levels. Nitrate and ammonium concentrations consistently increased with increasing PM_{2.5} while sulfate concentrations firstly increased but remained stagnant under high particulate conditions. The sulfur and nitrogen oxidation ratios exhibited relatively low values of 0.18 ± 0.12 and 0.11 ± 0.05 , respectively. Nitrogen oxidation ratio showed little dependence on relative humidity because of limited aqueous phase generation of nitrate. The increasing nitrate to sulfate ratio and decreasing organic carbon to elemental carbon ratio under high particulate concentrations indicate relative decreasing contribution of coal burning and increasing contribution of vehicle exhaust emissions on particulate pollution. The rapid decreasing trend of secondary organic carbon to elemental carbon ratio under high particulate concentrations was attributed to a combination of the relatively decreasing photochemical generations and increasing accumulation of primary emissions by the weakened atmospheric diffusion ability. Our results suggest that controlling primary carbonaceous species and vehicle exhaust emissions is the most effective measure in order to sustainably mitigate particulate pollution in Lanzhou in the future.

1. Introduction

Particulate matter (PM), primarily emitted or generated in the atmosphere, plays an important role in deteriorating air quality, altering weather and climate, and damaging human health (Chow et al., 2006; Dockery & Pope, 1994; Li et al., 2016). Particulate pollution has attracted widespread attentions across the world due to enhanced anthropogenic emissions in the last few decades (An et al., 2019; Fuzzi et al., 2015; Gartrell & Friedlander, 1975). China has experienced severe particulate pollution, and great efforts have been made to improve the air quality (Hsu et al., 2010; Li, Wang, et al., 2019; Tian et al., 2020; Zhang, Reid, et al., 2017). However, formation mechanisms of particulate pollution are complicated and vary with cities because of the varying emissions, meteorological conditions, as well as topography (Cao et al., 2013; Ding et al., 2016; Jiang et al., 2019; Quirin, 2020; Zheng et al., 2015).

The formation mechanisms of particulate pollution in world cities have been investigated in terms of primary emissions, secondary generation, and diffusion conditions (Huang et al., 2020; Thishan Dharshana et al., 2010; Venecek et al., 2019). Secondary generation of organic and inorganic aerosols is receiving increasing attention, especially in the most polluted cities in China (Shi et al., 2019; Wang et al., 2019; Wang, Wang, et al., 2020; Yao et al., 2018). Aqueous generation has been suggested to be a major contributor of sulfate and nitrate (Quan et al., 2014; Wang, Zhang, et al., 2016). The influence of photochemical conversion and heterogeneous reaction on nitrate and sulfate have also been studied. For example, sulfate forms primarily through atmospheric oxidation of SO₂ emitted mainly from coal burning, while nitrate originates from NO_x from vehicle exhaust and power plants (Huang et al., 2014; Wang et al., 2014). The secondary generation of organic aerosols is more challenging due to complex precursors and formation mechanisms (Sun et al., 2014; Xu et al., 2016; Xiao et al., 2020). The daytime nitrate and sulfate were mainly from

Writing - original draft: Tao Du, Min Wang, Xu Guan, Pengfei Tian

Writing - review & editing: Tao Du, Min Wang, Xu Guan, Min Zhang, Lei Zhang, Pengfei Tian, Jinsen Shi, Chenguang Tang

photochemistry while heterogeneous hydrolysis of N_2O_5 dominates the formation of nitrate and efficient heterogeneous reaction generated sulfate during nighttime (Li, Jacob, et al., 2019; Tian et al., 2019; Ye et al., 2019). In addition to the concentration of precursors, O_3 concentration, solar radiation, relative humidity (RH), and temperature were also important factors affecting the generation of secondary aerosols (Guo et al., 2020; Li et al., 2017).

Lanzhou, the capital city of Gansu province, is in the semiarid region in northwestern China. It is situated in a narrow river valley and surrounded by mountains, with an elevation of 1,500 to 2,000 m. Lanzhou has a population of 3.79 million in 2019 (Lanzhou Bureau of Statistics and Lanzhou Investigation team of National Bureau of Statistics, 2020) and covers an area of 13,083 km^2 . Lanzhou used to be one of the most polluted cities across the world due to heavy petrochemical industrial emissions (Tang & Li, 1989; Wang et al., 2009). Studies have investigated the mass loading of PM, chemical compositions from off-line filter samples, optical and radiative properties, influences of meteorological factors, potential sources, and control measures in Lanzhou during the last three decades. For example, concentrations of PM with different sizes in Lanzhou were studied in December 1999 ($\text{PM}_{2.5}$ and PM_{10}) (Liu et al., 2006), from October 1999 to April 2001 (PM_{10} and TSP) (Chu, Chen, Lu, Li, et al., 2008) and from January 2005 to February 2006 (PM_1 , $\text{PM}_{2.5}$, PM_{10} , and TSP) (Wang et al., 2009). The weak diffusion ability due to narrow and long valley topography and unfavorable meteorological conditions makes the pollution worse in Lanzhou, especially in winter with frequent temperature inversions, calm wind speed, and scant precipitation (RH) (Chu, Chen, & Lu, 2008). The influence of meteorological conditions on particulate pollution and their interactions have also been studied (Chen et al., 1993; Feng & Wang, 2012; Zhang et al., 2019). $\text{PM}_{2.5}$ ionic species were studied by samples collected from a suburban mountainous area of Lanzhou in summer 2006 (Pathak et al., 2009). Chemical composition and source apportionment of $\text{PM}_{2.5}$ have been studied based on offline filter samples collected in winter 2012 and summer 2013 and 2014 (Tan et al., 2017; Wang, Jia, et al., 2016). Control measures such as the reduction of bulk pollutant emissions, central heating, and the improvement of the ecological environment were suggested to improve air pollution in Lanzhou (An et al., 2008; Zhang et al., 2001; Zhang & Chen, 1994).

However, the formation mechanisms of particulate pollution in winter Lanzhou are still unclear due to a lack of key information such as the relative importance of photochemistry and aqueous phase reactions of secondary particulate pollutants, oxidation ratios of sulfur and nitrogen, the contributions of chemical species under different pollution levels, as well as characteristics of heavy particulate pollutions. The diurnal variation of chemical species in $\text{PM}_{2.5}$ is for the first time available in Lanzhou to study secondary pollutants generation by photochemistry and heterogenous reactions. Meanwhile, great efforts have been made to improve the air pollution in Lanzhou, especially since the 2013–2017 plan for Clean Air Action by Chinese government (The State Council of the People's Republic of China, 2013). Study on current characteristics and formation mechanisms of particulate pollution in Lanzhou can test the effectiveness of control measures in recent years. In addition, the air pollution in western China has increased in recent years but integrated researches were rarely available in this region.

The present study was designed to investigate the characteristics and formation mechanisms of winter particulate pollution in Lanzhou by using multiple online data, including chemical species, PM concentrations with different sizes, gases, and meteorological factors. The analysis was conducted under different severity of particulate pollutions with an emphasis on contribution of chemical species, formation of secondary inorganic aerosols, characteristic of carbonaceous species, as well as diurnal variation of chemical species. Our results will help to make effective control measures in Lanzhou and other cities in semiarid regions.

2. Data and Methodology

2.1. A Brief Introduction of the Station and Data

Field measurements were performed from 1 December 2019 to 9 February 2020 at the Lanzhou Atmospheric Components Monitoring Superstation (LACMS; 36.05°N, 103.87°E, 1520 m a.s.l.), which is settled on the roof of a 10-story building (approximately 20 m above the ground) on the campus of Lanzhou University (Figure 1). The LACMS station is a joint project between the Gansu Province Environmental Monitoring Center and Lanzhou University that is in the downtown area of Lanzhou city and surrounded by residential and business areas. Heavy petrochemical industries are situated in Xigu in the west suburb of Lanzhou city.

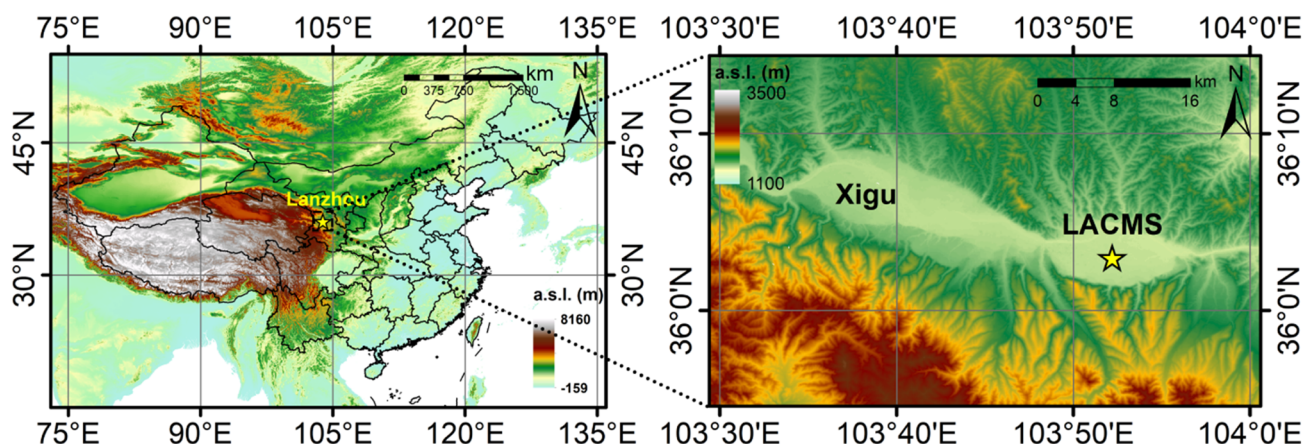


Figure 1. Geographical map and location of the LACMS station. The topographic data was the Shuttle Radar Topography Mission 3 (SRTM3) data from the National Aeronautics and Space Administration (NASA).

Multiple instruments were deployed to continuously measure the aerosol chemical compositions, PM concentrations with different sizes, gases, and meteorological parameters. An overview of online instruments is listed in Table S1 in the supporting information, and the details are presented in the following sections.

2.2. Particulate Matter

A particulate matter synchronous mixing monitor (5030i SHARP, Thermo Fisher, USA) was used to monitor the hourly mass concentrations of PM with an aerodynamic diameter of up to $1.0 \mu\text{m}$ (PM_{10}), $2.5 \mu\text{m}$ ($\text{PM}_{2.5}$), $10 \mu\text{m}$ (PM_{10}), and total suspended particles (TSPs) with a flow rate of $1 \text{ m}^3 \text{ hr}^{-1}$. The monitor applied light scattering method and β -ray absorption method for simultaneous monitoring. Digital filters were used for continuous quality calibration, and the filter belt was automatically updated according to settings. The instrument manual for installation, commissioning, and monitoring was strictly followed to ensure accurate and reliable data quality.

2.3. Water-Soluble Inorganic Ions

The hourly water-soluble inorganic ions (WSIIs; Cl^- , NO_3^- , SO_4^{2-} , NH_4^+ , Na^+ , K^+ , Mg^{2+} , and Ca^{2+}) in $\text{PM}_{2.5}$ were measured by a Monitor for AeRosols and Gases in ambient Air (MARGA, Applikon, The Netherlands), which is an advanced and widely used instrument across the world (Brink et al., 2019). Briefly, the MARGA consists of a sampling box, an analyzer box, and a control system. The inlet of MARGA employs a wet rotating denuder and a steam jet aerosol collector for collection of gases and particles, respectively. The gas and aerosol concentrations are reported in conjunction with a cation and anion chromatography at an hourly time resolution. The lowest detection limits of the detection components, including Cl^- , NO_3^- , SO_4^{2-} , NH_4^+ , Na^+ , K^+ , Mg^{2+} , and Ca^{2+} are 0.02, 0.05, 0.04, 0.05, 0.04, 0.09, 0.08, and $0.04 \mu\text{g m}^{-3}$, respectively. Details and principles of the MARGA can be found elsewhere (e.g., Makkonen et al., 2012; Rumsey et al., 2014). Excellent relationship between cations equivalents and anions equivalents in the present study demonstrated the high quality of the observed water-soluble ions (Figure S1).

The MARGA has already been used across the world and generally delivering satisfying results (Pye et al., 2018; Roig Rodelas et al., 2019; Twigg et al., 2015). The MARGA was compared with other reference methods to evaluate its performance, resulting in coefficients of determinations of 0.91 for the measurements against the SO_2 gas monitor, 0.84, 0.79, and 0.85 for the ACSM NO_3^- , SO_4^{2-} , and NH_4^+ measurements, respectively, and 0.85, 0.88, 0.91, and 0.86 for the filter measurements of Cl^- , NO_3^- , SO_4^{2-} , and NH_4^+ , respectively (Stieger et al., 2018). Moreover, online instruments can partially avoid the composition artifacts of filter-based sampling due to interparticle interactions, gas-particle interactions, and the dissociation of semivolatile species.

2.4. Carbonaceous Species

We applied an online and continuous particulate carbon monitor (Model 4/OCEC (RT-4) Lab, Sunset, USA) to measure the hourly organic carbon (OC) and elemental carbon (EC). The Sunset Lab OC/EC monitor adopts the thermal/optical method approved by NIOSH (The National Institute for Occupational Safety and Health) to measure and analyze OC and EC collected on the quartz filter membrane. For data quality assurance, we carried out a comparison between online data from Sunset Lab OC/EC monitor with the concentration of black carbon (BC) from the aethalometer (AE33, Magee, USA). A good correlation was found between the two methods even though EC was lower than BC (Figure S2), which might be attributed to overestimation of BC due to the absorption of dust and other absorbing aerosols (Salako et al., 2012).

OC can be divided into primary organic carbon (POC) and secondary organic carbon (SOC). Since POC and EC emissions were invariable for a short period and EC emissions are inert to atmospheric chemical reaction, the minimum OC/EC ratio method was applied to derive POC and SOC (Cao et al., 2007; Castro et al., 1999; Turpin & Huntzicker, 1991). Organic matter (OM) and SOC and were calculated as follows:

$$OM = 1.6 \times OC \quad (1)$$

$$SOC = OC_{total} - EC \times (OC/EC)_{min} \quad (2)$$

where $(OC/EC)_{min}$ is the minimum value of OC/EC ratio in the data.

2.5. Gaseous Pollutants and Meteorological Parameters

Concentrations of trace gases including O_3 , SO_2 , NO , NO_2 , and CO were obtained at a resolution of 1 hr using a set of online gas analyzers (49i, 43i, 42i, and 48i, respectively; Thermo Fisher Scientific, USA). Hourly meteorological parameters were collected by applying meteorological sensor (FWS500, FRT, China), including temperature (T), RH, air pressure (P), wind direction (WD), and wind speed (WS).

3. Particulate Pollution From Low to High PM Concentrations

3.1. Particulate Matter With Different Sizes

Average concentration of PM_{10} , $PM_{2.5}$, PM_{10} , and TSP during the 2019–2020 winter was 45.7 ± 20.9 , 70.4 ± 28.7 , 114 ± 47.8 , and $136.3 \pm 60.9 \mu g m^{-3}$, respectively (Table S2). Average ratios of PM_{10} to $PM_{2.5}$, $PM_{2.5}$ to PM_{10} , and $PM_{2.5}$ to TSP were 0.64, 0.62, and 0.53, respectively. $PM_{1-2.5}$, $PM_{2.5-10}$, and PM_{10+} were calculated to better characterize the variation of PM with different sizes. The total observation samples were divided into 10 particulate pollution bins based on $PM_{2.5}$ which is of widespread attention. PM_{10} and $PM_{1-2.5}$ continuously increased from low to high PM concentrations while $PM_{2.5-10}$ and PM_{10+} showed little variation under low PM concentrations and began to increase at about $65 \mu g m^{-3} PM_{2.5}$ concentration (Figure 2a). The ratio of PM_{10} to $PM_{2.5}$ generally increased from 0.60 to 0.69 with increasing PM concentration (Figure 2b), indicating greater contribution of submicron aerosols under high PM concentrations. The ratio of $PM_{2.5}$ to PM_{10} firstly increased and began to decrease at about $65 \mu g m^{-3} PM_{2.5}$ concentration.

Lanzhou used to be a heavily polluted city with average PM_{10} , $PM_{2.5}$, PM_{10} , and TSP of 161.5, 164.9, 460.5, and $726.2 \mu g m^{-3}$, respectively during December 2005 (Wang et al., 2009). $PM_{2.5}$ concentration in Lanzhou was $120.5 \mu g m^{-3}$ during December 2012 (Tan et al., 2017) and $141.1 \mu g m^{-3}$ for 2014 winter (Wang, Jia, et al., 2016). Average PM_{10} was $57.3 \mu g m^{-3}$ during January to February 2014 (Xu et al., 2016). The air quality in Lanzhou has been greatly improved under strict control measures in the last three decades. The current winter particulate pollution in Lanzhou is also much lower than cities in eastern China (e.g., Sun et al., 2020; Ye et al., 2019).

The PM_{10} to $PM_{2.5}$ and $PM_{2.5}$ to PM_{10} ratios during 2019–2020 winter in Lanzhou (0.64 and 0.62) are consistent with the spatial distribution of PM ratios across China with low values in north and northwest China (Wang et al., 2015). Besides spatial differences, the ratios of PM with different sizes vary during pollution events. For example, the ratio of PM_{10} to $PM_{2.5}$ decreased during winter haze episodes in Xi'an and Beijing (Elser et al., 2016), which is opposite to the trends of PM_{10} to $PM_{2.5}$ ratio for high PM concentrations in the present study. The increasing trend of PM_{10} to $PM_{2.5}$ ratio might be attributed to strong photochemical

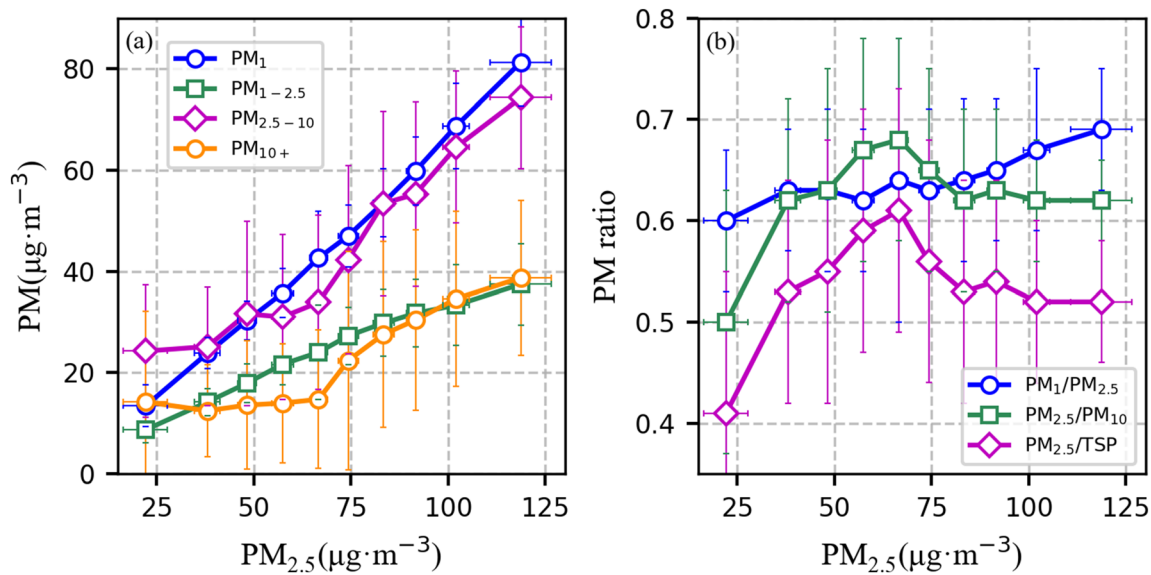


Figure 2. Concentrations (a) and ratios (b) of PM with different sizes from low to high pollution concentrations. The 1,663 observation samples were divided into 10 bins from low to high $PM_{2.5}$ concentrations with each bin contains 166 or 167 samples. $PM_{1-2.5}$, $PM_{2.5-10}$, and PM_{10+} represents the differences between $PM_{2.5}$ and PM_1 , PM_{10} and $PM_{2.5}$, and TSP and PM_{10} , respectively.

generation of secondary aerosols under dry conditions, which will be further illustrated in the following sections.

3.2. Contribution of Chemical Species

OM and the secondary inorganic aerosols (SIAs; i.e., nitrate, sulfate, and ammonium) were the major compositions of $PM_{2.5}$ during 2019–2020 winter in Lanzhou (Figure 3). Average value of OM concentration was $25.2 \mu\text{g m}^{-3}$ for the total winter samples, contributed the highest mass fraction of 35.8% in $PM_{2.5}$. Nitrate

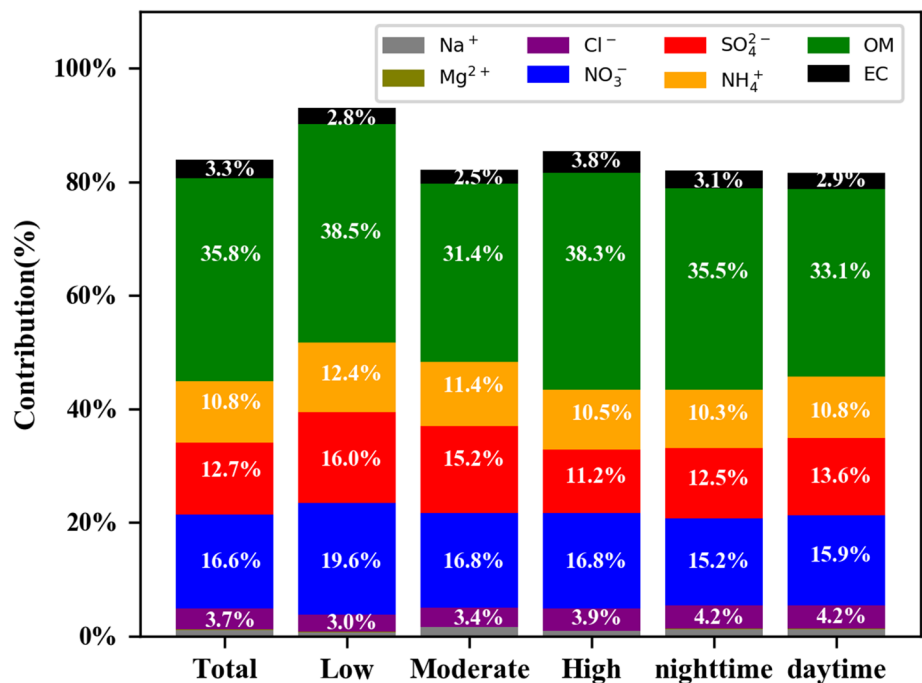


Figure 3. $PM_{2.5}$ compositions for total, low, moderate, and high pollution levels, as well as nighttime (02:00, 03:00, 04:00, and 05:00) and daytime (12:00, 13:00, 14:00, and 15:00) samples.

($11.7 \mu\text{g m}^{-3}$), sulfate ($8.9 \mu\text{g m}^{-3}$), and ammonium ($7.6 \mu\text{g m}^{-3}$) accounted for 16.6%, 12.7%, and 10.8%, respectively, of $\text{PM}_{2.5}$ mass. The combination of OM and SIAs accounted for 75.9% of $\text{PM}_{2.5}$ mass. The average concentrations of Cl^- and EC were 2.6 and $2.3 \mu\text{g m}^{-3}$, accounted for 3.7% and 3.3% of $\text{PM}_{2.5}$ mass. The average concentrations of K^+ , Na^+ , Ca^{2+} , and Mg^{2+} were 0.88 , 0.75 , 0.41 , and $0.06 \mu\text{g m}^{-3}$, respectively. The undetected $\text{PM}_{2.5}$ mass might be mineral dust component. The contributions of carbonaceous species (OM and EC; 39.1%) is comparable with those of SIAs (40.1%).

To better understand the contribution of chemical species, the observations in the present study were grouped into low (daily $\text{PM}_{2.5} \leq 35 \mu\text{g m}^{-3}$), moderate ($35 < \text{daily PM}_{2.5} \leq 75 \mu\text{g m}^{-3}$), and high (daily $\text{PM}_{2.5} \geq 75 \mu\text{g m}^{-3}$) pollution levels. The days of low, moderate, and high pollution levels accounted for 8%, 47%, and 45%, respectively, during the 2019–2020 winter in Lanzhou. The minimum, median, and maximum value of daily $\text{PM}_{2.5}$ during the 2019–2020 winter was 18.23 , 67.22 , and $116.36 \mu\text{g m}^{-3}$, respectively. Average $\text{PM}_{2.5}$ concentration under low, moderate, and high pollution levels was 28.2 , 54.5 , and $93.7 \mu\text{g m}^{-3}$, respectively.

The mass fractions of OM in $\text{PM}_{2.5}$ were 38.5%, 31.4%, and 38.3% for low, moderate, and high pollution levels, respectively (Figure 3). The lowest contribution of OM was found for the moderate pollution level even though OM concentration for the moderate pollution level was 1.58 times of that for low pollution level (Table S2). From low to high pollution level, the concentrations of nitrate, sulfate, and ammonium were multiplied by 2.8, 2.3, and 2.8 times, respectively. However, the contributions of SIAs decreased from low to high pollution level with the mass fractions of nitrate (sulfate and ammonium) in $\text{PM}_{2.5}$ were 19.6% (16.0% and 12.4%), 16.8% (15.2% and 11.4%), and 16.8% (11.2% and 10.5%), respectively for low, moderate, and high pollution levels. The reduction in mass fraction of sulfate (4.8%) was higher than those of nitrate (2.8%) and ammonium (1.9%). The contributions of chloride and EC were relatively low, but their concentrations significantly increased from low to high pollution level. The concentrations of chloride and EC for the high pollution level (3.70 ± 2.13 and $3.53 \pm 1.45 \mu\text{g m}^{-3}$) were 4.35 and 4.47 times of those for the low pollution level (0.85 ± 0.61 and $0.79 \pm 0.36 \mu\text{g m}^{-3}$). The contributions of carbonaceous species (OM and EC) were 41.3%, 33.8%, and 42.3% while those of SIAs were 48.0%, 43.4%, and 38.5% for low, moderate, and high pollution levels, respectively. In other words, the contribution of SIAs was higher than carbonaceous species for low pollution level while carbonaceous species became the major contributor for the high pollution level due to relative increase in the contribution of carbonaceous species and decrease contribution of SIAs.

The contributions of chemical species during 2019–2020 winter in Lanzhou are generally within the scope of studies in other cities (Beijing, Xi'an, Shanghai, and Guangdong) across China (Huang et al., 2014). The nitrate contribution of 16.6% is relatively higher, indicating the importance of mobile sources. Significant increase in nitrate, evident decrease in sulfate, and slight increase in ammonium were found between 2019 and 2020 winter (nitrate: $11.7 \mu\text{g m}^{-3}$, sulfate: $8.9 \mu\text{g m}^{-3}$, and ammonium: $7.6 \mu\text{g m}^{-3}$; the present study) and previous studies in Lanzhou such as summer 2006 (nitrate: $3.2 \pm 2.0 \mu\text{g m}^{-3}$, sulfate: $9.8 \pm 5.6 \mu\text{g m}^{-3}$, and ammonium: $4.1 \pm 2.5 \mu\text{g m}^{-3}$) (Pathak et al., 2009) and December 2012 (nitrate: $7.21 \pm 4.08 \mu\text{g m}^{-3}$, sulfate: $11.82 \pm 4.21 \mu\text{g m}^{-3}$, and ammonium: $6.70 \pm 3.42 \mu\text{g m}^{-3}$) (Tan et al., 2017). The contribution of SIAs in Lanzhou is lower than megacities such as Nanjing (61%) (Zhang, Tang, et al., 2017), Chengdu (51.04%) (Liu et al., 2019), and Changzhou (51.81%) (Ye et al., 2019). Low contribution of SIAs was also found in some cities, for instance, Yulin during 2013–2014 (24.46%) (Lei et al., 2020) and Shijiazhuang during 2014–2016 (32.01%) (Xie et al., 2019).

3.3. Formation of Secondary Inorganic Aerosols

Sulfate, nitrate, and ammonium increased with increasing particulate pollution when $\text{PM}_{2.5}$ concentration was lower than $65 \mu\text{g m}^{-3}$ (Figure 4a). Sulfate showed little variation at about $10.3 \mu\text{g m}^{-3}$ with increasing $\text{PM}_{2.5}$ when the concentration of $\text{PM}_{2.5}$ was higher than $65 \mu\text{g m}^{-3}$. Nitrate (ammonium) increased from 4.7 (3.1) $\mu\text{g m}^{-3}$ for the lowest $\text{PM}_{2.5}$ bin to 18.9 (11.4) $\mu\text{g m}^{-3}$ for the highest $\text{PM}_{2.5}$ bin. The mole ratio of nitrate to sulfate was investigated to better understand the relative contribution of mobile (i.e., vehicles exhaust) and stationary sources (Figure 4b). In general, high $[\text{NO}_3^-]/[\text{SO}_4^{2-}] (>1)$ indicated that the predominance of vehicle exhaust over coal combustion sources (Kato, 1996; Wang et al., 2006). Average nitrate to sulfate ratio during winter 2019–2020 in Lanzhou was 2.03, indicating high contribution of vehicle exhaust

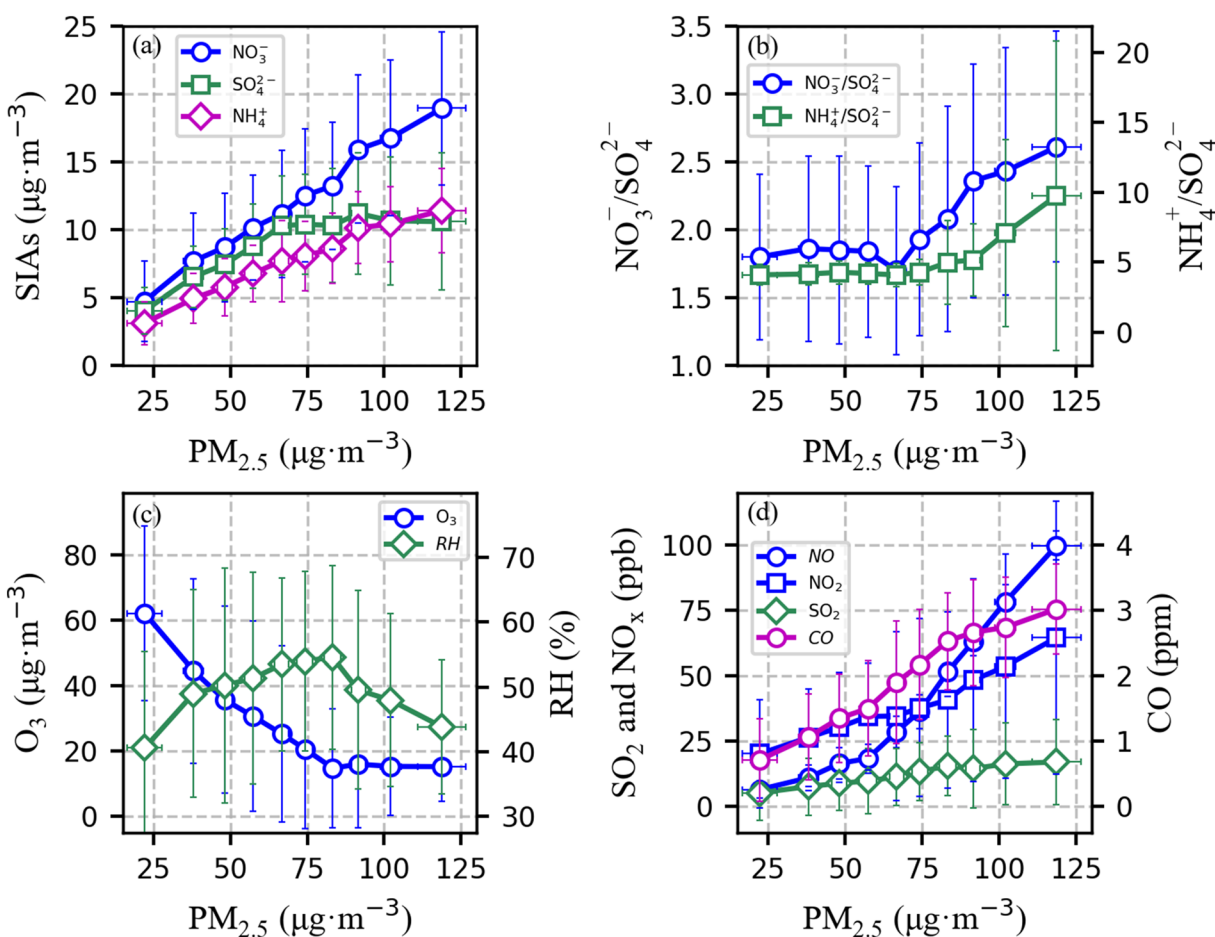


Figure 4. SIAs (a), mole ratios of nitrate to sulfate and ammonium to sulfate (b), ozone and relative humidity (c), and SO_2 , NO_x , and CO (d) as a function of $PM_{2.5}$.

emissions. The nitrate to sulfate ratio began to increase with $PM_{2.5}$ when $PM_{2.5}$ was higher than $65 \mu\text{g m}^{-3}$, indicating increasing contribution of vehicle exhaust emissions on particulate pollution for high particulate pollution conditions during winter in Lanzhou.

The sulfur and nitrogen oxidation ratios (SOR and NOR) are generally used to infer the degree of atmospheric secondary transformation of SO_2 and NO_2 to sulfate and nitrate, which were calculated by the following equations:

$$\text{SOR} = [\text{SO}_4^{2-}] / ([\text{SO}_4^{2-}] + [\text{SO}_2]) \quad (3)$$

$$\text{NOR} = [\text{NO}_3^-] / ([\text{NO}_3^-] + [\text{NO}_2]) \quad (4)$$

where $[\text{SO}_4^{2-}]$ and $[\text{NO}_3^-]$ are the molar concentrations ($\mu\text{mol}\cdot\text{m}^{-3}$) in $PM_{2.5}$ and $[\text{SO}_2]$ and $[\text{NO}_2]$ are the molar concentrations ($\mu\text{mol}\cdot\text{m}^{-3}$) in gas phase. SOR and NOR values of higher than 0.1 indicate secondary generation of sulfate and nitrate (Fu et al., 2008; Ohta & Okita, 1990). The average SOR and NOR during winter 2019–2020 in Lanzhou were 0.18 ± 0.12 and 0.11 ± 0.05 , respectively. SOR exhibited decreasing trend under high $PM_{2.5}$ conditions while NOR showed little variation from low to high $PM_{2.5}$ concentrations (Figure 5a). The stagnant of sulfate under high $PM_{2.5}$ conditions was attributed to the reduction of SOR, which was probably caused by a decline in heterogeneous reactions and the reduced photochemical conversion of SO_2 . Under high $PM_{2.5}$ conditions, the decline in heterogeneous reactions was evident in declining trend of RH and the photochemistry was reduced due to lowered O_3 concentration (Figure 4c). The formation of nitrate during winter 2019–2020 in Lanzhou seems to be determined mainly by NO_x concentrations because of the rapid increasing of NO_x concentrations and stagnant low values of

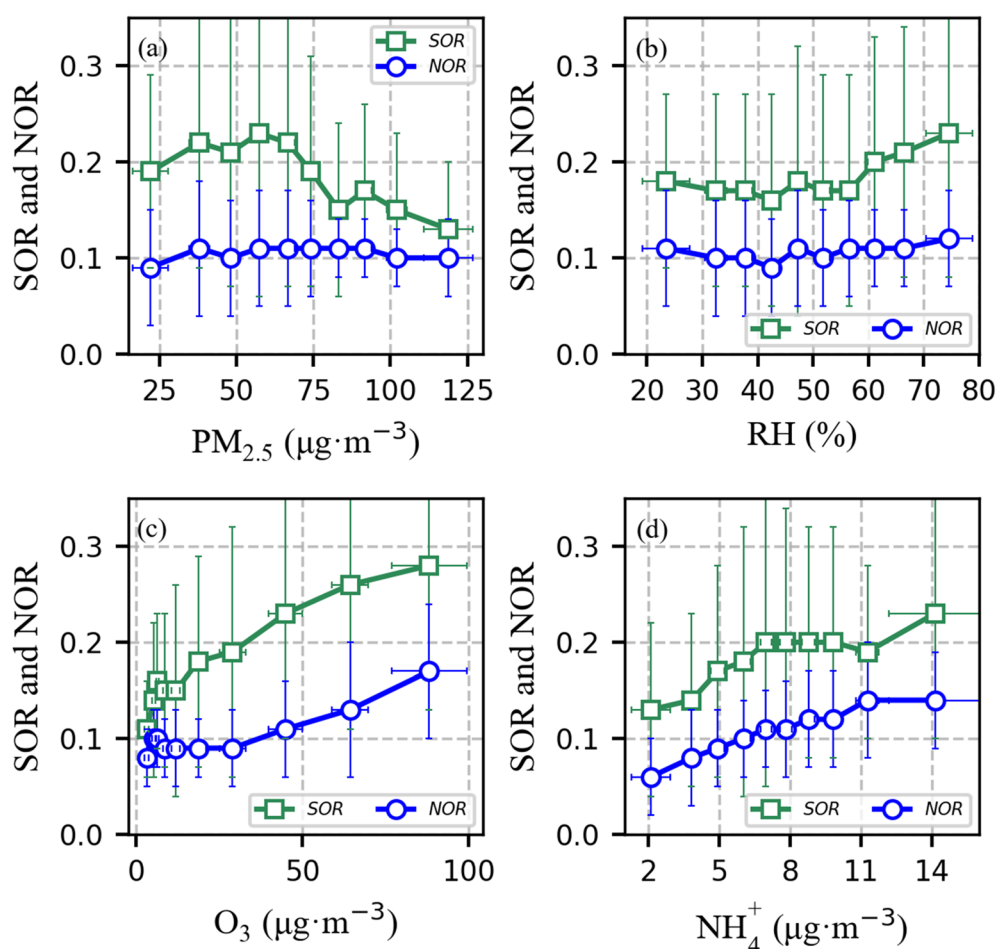


Figure 5. SOR and NOR as a function of $PM_{2.5}$ (a), RH (b), O_3 (c), and ammonium (d). Similar to the division of $PM_{2.5}$, the total samples were divided into 10 bins from low to high RH/ O_3 /ammonium concentrations.

NOR. Note that the increasing rates of NO concentration with increasing $PM_{2.5}$ were much higher than those of NO_2 and SO_2 concentrations from low to high $PM_{2.5}$ concentrations (Figure 4d). The ratio of NO concentration for high pollution level to that of low pollution level was 10.7 while those of NO_2 and SO_2 were both 2.5.

The relationships between SOR/NOR and possible influential factors were investigated to better understand the formation of SIAs (Figure 5). NOR was significantly lower than SOR under various conditions during the 2019–2020 winter in Lanzhou. SOR and NOR showed little variation with increasing RH when RH was lower than 50%. When RH was above 50%, the SOR started to increase with increasing RH while NOR still exhibited weak variation with increasing RH. That is, SOR was more sensitive to RH than NOR under high RH conditions (also in Figure S6). No apparent trend for SOR and NOR as a function of O_3 concentrations was found under low O_3 concentrations of lower than $20 \mu\text{g m}^{-3}$. SOR and NOR rapidly increased with increasing O_3 concentrations when O_3 concentrations were higher than $20 \mu\text{g m}^{-3}$, indicating sensitive photochemical generation of sulfate and nitrate. SOR and NOR generally increased from low to high ammonium concentrations. Combining the relationships between SOR/NOR and RH and O_3 , it's safe to conclude that formation of sulfate was a combination of heterogeneous reactions and the photochemical conversion of SO_2 while nitrate was mainly originated from NO_x photochemistry. Considering that SOR was more sensitive to RH than NOR under high RH conditions, the decrease of SOR under high PM conditions was reconfirmed to be caused by a decline in heterogeneous reactions and the reduced photochemical conversion of SO_2 . With the increasing of $PM_{2.5}$, decreasing O_3 concentration caused lower NOR while increasing ammonium resulted in higher NOR, leading to a stagnant NOR from low to high $PM_{2.5}$ concentrations.

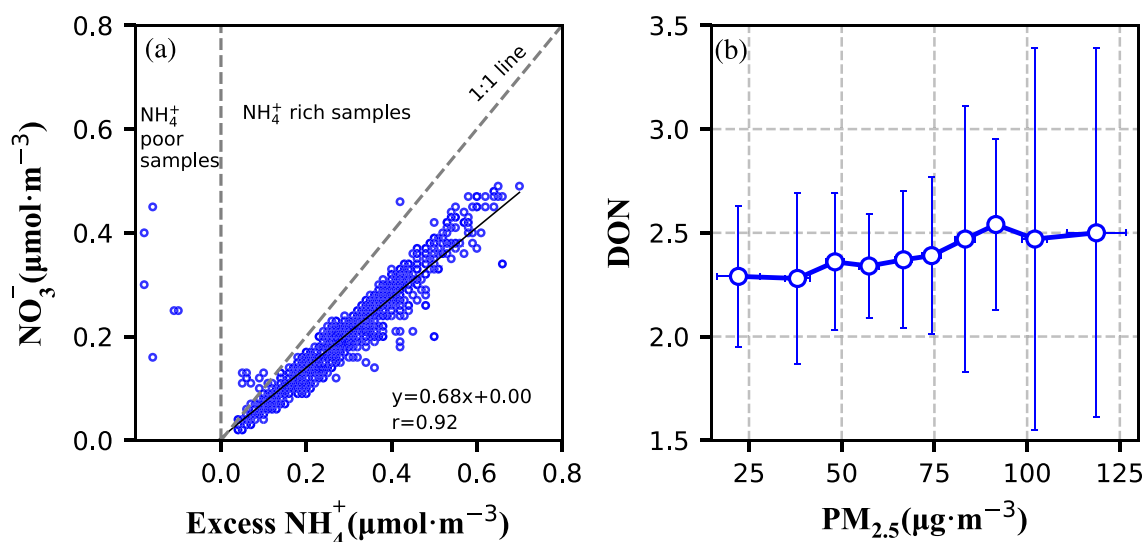


Figure 6. Nitrate as a function of excess ammonium (a) and DON as a function of $PM_{2.5}$ (b).

The correlation analysis of WSIs in $PM_{2.5}$ was conducted to investigate the potential relationships among WSIs and preliminarily deduce the existence form and source of the WSIs (Table S4). Both H_2SO_4 and HNO_3 react with NH_3 to form salts, and NH_3 is preferential to react with H_2SO_4 to form NH_4HSO_4 or $(NH_4)_2SO_4$. If NH_3 is enough for H_2SO_4 , then the excess NH_3 react with HNO_3 to form NH_4NO_3 . In fact, “excess ammonium” is defined as the amount of ammonium in excess of that required for $[NH_4^+]/[SO_4^{2-}] = 1.5$ (Pathak et al., 2009):

$$\text{Excess } [NH_4^+] = ([NH_4^+]/[SO_4^{2-}] - 1.5) \times [SO_4^{2-}] \quad (5)$$

where $[SO_4^{2-}]$, $[NO_3^-]$, and $[NH_4^+]$ are the molar concentrations ($\mu\text{mol}\cdot\text{m}^{-3}$) in $PM_{2.5}$. When the “excess ammonium” is >0 , homogenous gas-phase formation of nitrate is significant. The ammonium rich samples accounted for 99.6% of the total samples (Figure 6a). The aerosol acidity in Lanzhou was low (Figure S7). Good linear relationship was found between nitrate and excess ammonium with $R^2 = 0.92$, conforming the formation of nitrate from homogeneous gas-phase reaction between ammonia and nitric acid during winter in Lanzhou (also in Figures S4 and S5).

The degree of sulfate neutralization (DON) was employed to estimate whether sulfate was completely acidic, fully neutralized by ammonia, or in between, which is defined as follows:

$$\text{DON} = ([NH_4^+] - [NO_3^-])/[SO_4^{2-}] \quad (6)$$

where the $[SO_4^{2-}]$, $[NO_3^-]$, and $[NH_4^+]$ are the molar concentrations ($\mu\text{mol}\cdot\text{m}^{-3}$) in $PM_{2.5}$. If sulfate were fully neutralized in the form of ammonium sulfate, that would mean 2 mol ammonia for every mole of sulfate and the DON value could be defined as 2. Similarly, DON was 1 when sulfate was ammonium bisulfate, and DON was 0 when sulfate was particulate sulfuric acid (Chen et al., 2014; Qiu et al., 2016). Average DON value during 2019–2020 winter in Lanzhou was 2.4, indicating the that sulfate was in the form of ammonium sulfate. DON generally increased with $PM_{2.5}$ under high particulate pollution conditions (Figure 6b).

3.4. Characteristics of Carbonaceous Species

Generally, EC, POC, and SOC increased from low to high $PM_{2.5}$ concentrations during 2019–2020 winter in Lanzhou (Figure 7a). EC (POC; SOC) increased from 0.7 (1.5; 3.8) $\mu\text{g m}^{-3}$ in the lowest $PM_{2.5}$ bin to 4.8 (10.7; 17.2) $\mu\text{g m}^{-3}$ in the highest $PM_{2.5}$ bin. The correlation of OC and EC was studied to better understand the sources of carbonaceous species in PM (Figure S3). The correlation of OC and EC was high with $R^2 = 0.91$ for the total samples and the correlations showed little variation with increasing $PM_{2.5}$, indicating that OC and EC originated from the same sources from low to high $PM_{2.5}$ concentrations.

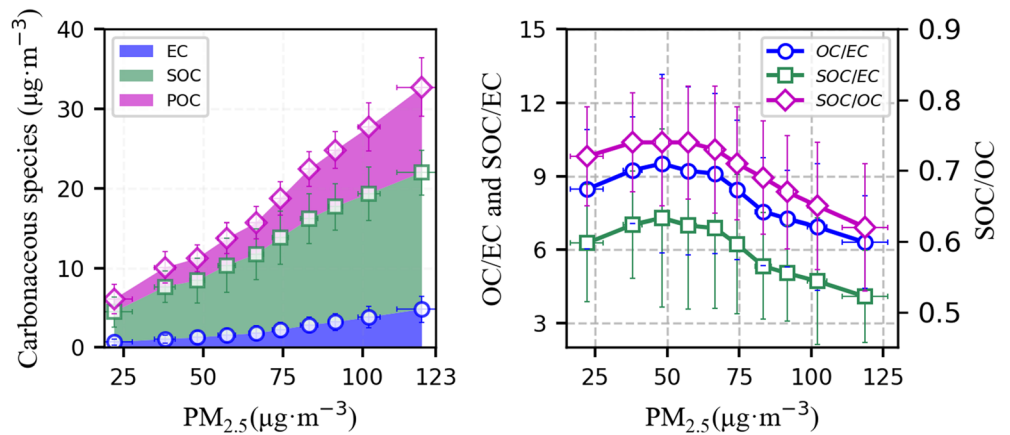


Figure 7. Variation of EC, POC, and SOC (a) and the ratios of OC to EC, SOC to OC, and SOC to EC (b) as a function of $PM_{2.5}$.

The ratio of OC to EC is an indicator for relative contribution of different sources of carbonaceous species: 0.3–7.6 for emissions from coal burning, 0.7–2.4 for exhaust emissions from diesel and gasoline vehicles, and 4.1–14.5 for emissions from biomass burning (Turpin & Huntzicker, 1991; Watson et al., 2001). The OC/EC ratios in above studies were measured following the IMPROVE TOR (Interagency Monitoring of Protected Visual Environments, Thermal Optical Reflectance) protocol, whereas the OC/EC ratios in this study were measured following the NIOSH TOT (the National Institute for Occupational Safety and Health, Thermo Optical Transmission) protocol. The OC (EC) measured under the NIOSH protocol would be larger (smaller) than under the IMPROVE protocol due to different temperatures for OC and EC (Cao et al., 2007). Although the NIOSH protocol led to larger OC/EC values, the OC/EC ratios can estimate the major sources of the particulate pollution (e.g., Chen et al., 2017; Qu et al., 2009). The average ratio of OC to EC was 8.2 for the total samples (Table S2). Since biomass burning is limited during winter in Lanzhou (Figure S8), the average OC to EC ratio of 8.2 indicated the greater contribution of coal burning than vehicle exhaust emissions. Results from offline samples also suggested that the major sources of carbonaceous aerosols in Lanzhou were coal burning and vehicle exhaust emissions (Wang, Jia, et al., 2016). The OC to EC ratio increased from 8.5 to 9.5 in the lowest three $PM_{2.5}$ bins and then began to decrease with increasing $PM_{2.5}$ and reached a minimum value of 6.3 in the highest $PM_{2.5}$ bin (Figure 7b). The decreasing trend of OC to EC ratio under high $PM_{2.5}$ concentrations demonstrated the relatively decreasing contribution of coal burning and increasing contribution of vehicle exhaust emissions on carbonaceous species.

The ratios of SOC to OC and SOC to EC were also studied to illustrate the characteristics of secondary carbonaceous species from low to high $PM_{2.5}$ concentrations (Figure 7b). Average SOC to OC ratio for total samples during 2019–2020 winter in Lanzhou was 68%, much higher than those observed in megacities such as Beijing for 2016–2017 winter (44%) (Shao et al., 2018) and Nanjing for 2015 winter (36%) (Zhang, Tang, et al., 2017). High ratios of SOC to OC have also been recorded in other cities, for instance, Zhengzhou for 2012 autumn ($60 \pm 8\%$) (Wang, Li, et al., 2016). The SOC to OC ratio decreased with $PM_{2.5}$ concentrations when $PM_{2.5}$ concentrations were higher than $50 \mu\text{g m}^{-3}$, indicating decreased photochemical formations of SOC. The minimum SOC to OC ratio in the highest $PM_{2.5}$ bin was as high as 62%. The decreasing trend of SOC to OC ratio in the present study seemed to be opposite to the results during winter in Beijing, where SOC to OC ratio was higher during haze events than clean conditions (Shao et al., 2018). Furthermore, the ratio of SOC to EC decreased rapidly from 7.2 to 4.1 with increasing $PM_{2.5}$ under high $PM_{2.5}$ concentrations. The rapid decreasing trend of SOC to EC ratio under high PM concentrations was attributed to a combination of decreasing secondary photochemical formations by reduced O_3 and the increasing accumulation of primary particulate emissions by weakened atmospheric diffusion ability (see wind speed as a function of $PM_{2.5}$ in Figure 9a).

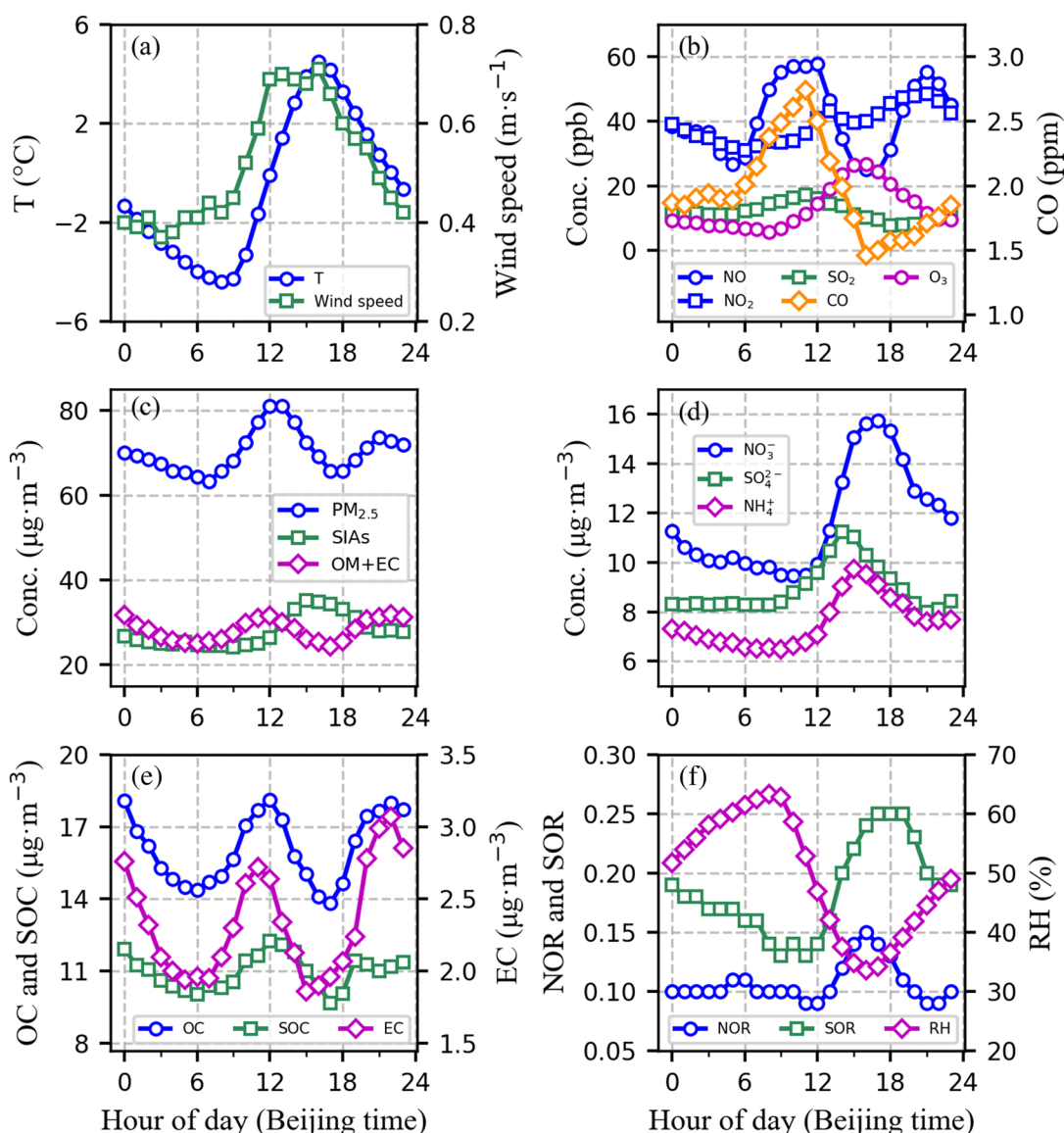


Figure 8. Diurnal variation of meteorological parameters (a), gases (b), PM (c), SIA (d), carbonaceous species (e), and NOR/SOR (f) for total samples during 2019–2020 winter in Lanzhou.

4. Discussions

4.1. Diurnal Variation of Particulate Pollution

To better understand the formation of particulate pollution, the diurnal variation of PM species, gases, NOR and SOR, and meteorological parameters was investigated. Typical diurnal variation of temperature and RH was found for 2019–2020 winter in Lanzhou (Figures 8a and 8g), with maximum temperature (minimum RH) at 16:00 and minimum temperature (maximum RH) at 08:00. The diurnal variation of RH was confined in the range of 30–65%, such low RH was unfavorable for aqueous phase reactions in the atmosphere. Relatively high wind speed in the afternoon (12:00–16:00) and low wind speed at midnight were observed (Figure 8a). The concentration of NO began to increase in the early morning and reached the first peak at 12:00, then evolved to a bottom at 16:00 and reached the second peak at 21:00 (Figure 8b). CO exhibited a peak at 11:00 and a bottom at 16:00. The peaks of CO and NO were attributed to anthropogenic activities, for instance, vehicle emissions. Ozone diurnal variation was controlled by solar radiation and reached one peak at 16:00. NO₂ reached the first peak at 13:00 and kept at a high level until midnight. SO₂ exhibited a single peak at 11:00.

The diurnal variation of $PM_{2.5}$ was like that of NO_x , with two peaks at 12:00 and 21:00 and two bottoms at 07:00 and 18:00 (Figure 8c). One evident peak at 15:00 was found for SIAs and two peaks for carbonaceous species were at 12:00 and 22:00, respectively. Single sharp peaks were found for nitrate, sulfate, and ammonium at 17:00, 14:00, and 15:00, respectively. Not only SIAs but also NOR and SOR during daytime were significantly higher than those in nighttime. Since the NO_x concentrations were very high, the diurnal variation of nitrate seemed to be controlled by the diurnal variation of NOR (Figure 8f). The nighttime NOR was at a low value of about 0.1, indicating little secondary generation of nitrate during nighttime. NOR started to increase at 12:00 and reached a peak value at 16:00, leading to the peak of nitrate at 17:00. Note the slight increase in NOR at 05:00 also triggered a minor fluctuation of nitrate, which was produced by the hydrolysis of N_2O_5 at night with relative high RH. SOR increased while SO_2 decreased from 11:00 to 19:00, resulting in the sulfate peak at 16:00. Decreasing trends were found for nitrate, ammonium, and carbonaceous species while sulfate remained stagnant from midnight to sunrise. The decrease of various species during nighttime was caused by diffusion, and the stagnant of sulfate indicated generation of sulfate via aqueous phase reactions during nighttime. Like $PM_{2.5}$, there were also two peaks for OC and EC with the first ones at 12:00 and the second ones at 22:00 (Figure 8c), indicating the primary emission of carbonaceous species by anthropogenic activities, for instance, vehicle emissions. SOC exhibited an evident peak at 12:00 and kept high values from 19:00 to midnight. To sum up, SIAs diurnal variations conform that the formation of SIAs were dominated by daytime photochemistry rather than heterogeneous reactions in 2019–2020 winter in Lanzhou.

The correlation coefficients between NOR/SOR and O_3 and RH were investigated to better understand the relative importance of photochemistry and aqueous generation of sulfate and nitrate (Table S3). The correlation coefficient between NOR (SOR) and O_3 was 0.51 (0.44) while that between NOR (SOR) and RH was 0.08 (0.14), which reconfirming the dominance contribution of photochemical generation of sulfate and nitrate rather than aqueous phase conversion.

Contributions of chemical species for selected daytime samples and selected nighttime samples were also studied to further compare photochemistry and heterogeneous reactions during winter in Lanzhou. The average $PM_{2.5}$ for the selected daytime and nighttime samples were 78 and 67 $\mu g m^{-3}$, respectively. The contributions of nitrate, sulfate, and ammonium for daytime samples were all higher than those for nighttime ones (Figure 3). The increased contribution of SIAs for daytime samples was attributed to higher secondary generation of nitrate, sulfate, and ammonium. The contribution of carbonaceous species for daytime samples was lower than those for nighttime samples, which were partially due to the higher diffusion of primary carbonaceous species and relatively higher SIAs during daytime.

4.2. Influence of Meteorological Factors on Particulate Pollution

Meteorological factors affect atmospheric particulate pollution by influencing diffusion conditions and secondary aerosol generation. The influence of RH on secondary aerosol generation has also been investigated in previous sections. Hourly RH varied from 10.7% to 87.8%, with an average value of 49.5% during 2019–2020 winter in Lanzhou. Such low RH was unfavorable for aqueous phase convention of secondary aerosols in the atmosphere. Since wind speed is a good indicator for diffusion conditions, the relationship between wind speed and $PM_{2.5}$ concentration was also investigated. The average wind speed was only 0.52 $m s^{-1}$ for total samples during 2019–2020 winter in Lanzhou. Low wind speed indicated weak pollution diffusion ability during winter in Lanzhou due to valley topography and unfavorable meteorological factors such as shallow boundary layer and frequent temperature inversion. Generally, wind speed decreased rapidly with increasing $PM_{2.5}$ from 0.79 $m s^{-1}$ for the lowest $PM_{2.5}$ bin to 0.44 $m s^{-1}$ for the highest $PM_{2.5}$ bin (Figure 9a), confirming the increasing accumulation of pollution by weakening diffusion ability under high PM conditions. In addition, weak diffusion ability under high PM conditions might have been caused by reduced solar radiation due to elevated particulate pollution.

The prevailing winds came from the north direction during 2019–2020 winter at the LACMS station (Figure 9b). The eastern winds with relatively high speed were favorable while the northern and western winds with relatively low speed were unfavorable for pollution diffusion. The influence of wind on pollutions was studied in detail for low, moderate, and high pollution levels (Figure S9). Obviously, the low pollution level was accompanied by eastern winds with relatively high wind speed. Winds from northern, eastern, and western were comparable for the moderate pollution level. For the high pollution level, low speed winds

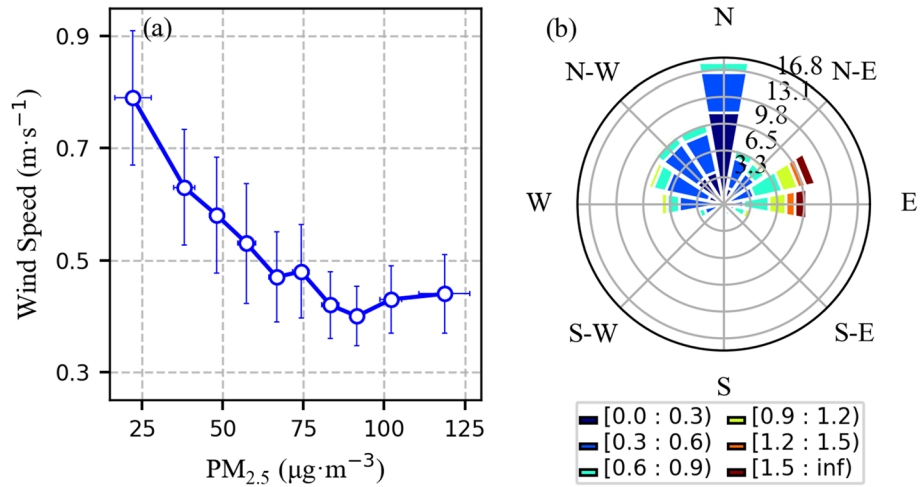


Figure 9. Wind speed as a function of PM_{2.5} (a) and wind rose plot (b).

blew from northern and western directions with high particulate and gaseous pollutions. Since Lanzhou is an isolated city, which is settled in a narrow river valley and surrounded by mountains, regional transport of particulate pollution was not studied due to its small order of magnitude in winter.

4.3. Variations of PM and Gases During Recent Years in Lanzhou

Variations of PM₁₀, SO₂, and NO₂ were studied to reveal the trend of air pollution in Lanzhou from 2002 to 2019. PM_{2.5} data was also available for recent 6 years. The decrease trend was evident in PM₁₀ and SO₂ during the last two decades, and a slight decrease was also found for PM_{2.5} since 2014, which might be a consequent result of the Clean Air Action by Chinese government. The yearly average of SO₂ in 2019 was only

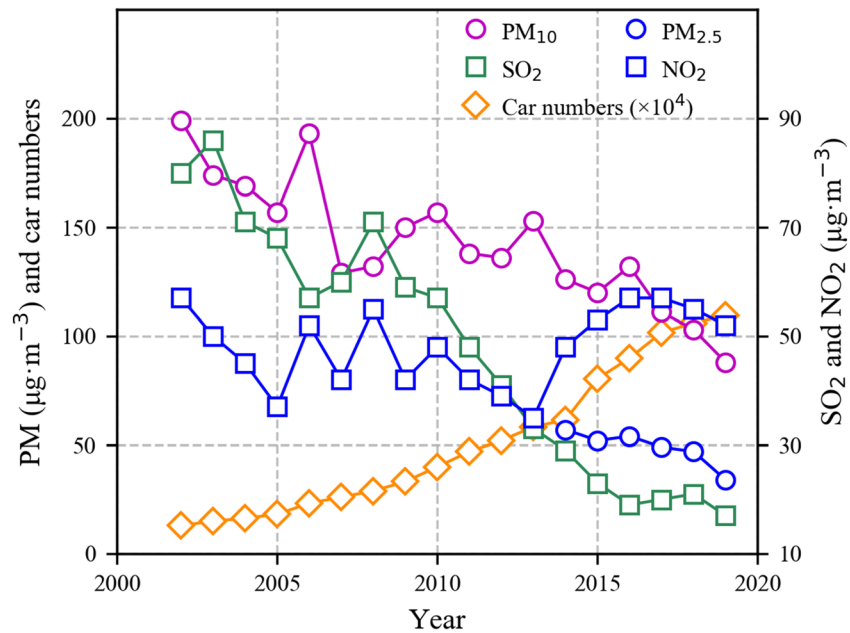


Figure 10. PM_{2.5}, PM₁₀, SO₂, NO₂, and car numbers during recent years in Lanzhou. The data of PM_{2.5} and gases were obtained from the China National Environmental Monitoring Center (CNEMC) website (<http://113.108.142.147:20035/emcpublish/>) for the site of Lanzhou Railway Institute, which is about 1,500 m away from the LACMS station. SO₂, NO₂, and PM₁₀ data was from Lanzhou City's State of the Environment bulletins distributed by Lanzhou Ecology and Environment Bureau (<http://sthjj.lanzhou.gov.cn/>). The car numbers were from Lanzhou City's Economic and Social Development Statistics Bulletins distributed by Lanzhou Municipal Bureau of Statistics (<http://www.tjcn.org/>).

21.2% of that in 2002, indicating effective control on SO₂ in Lanzhou. However, the concentration of NO₂ in 2019 (52 μg m⁻³) was close to that in 2002 (57 μg m⁻³). The increase trend of NO₂ in Lanzhou is contrast to the decrease trend of NO₂ across China from 2013 to 2017 (Wang, Gao, et al., 2020). That is, unfortunately, the control measures failed to reduce the vehicle exhaust emissions in Lanzhou.

Coal combustion, soil dust, and traffic emissions were identified as the highest three sources (accounted for 65.8%) in Lanzhou (Wang, Jia, et al., 2016). Traffic emissions seem to be increased in recent years due to the increase trend of NO₂ since 2013. Meanwhile, the car ownership in Lanzhou has grown from 0.13 million in 2002 to 1.10 million by the end of 2019. Measures such as promote vehicle restriction policies, increase the coverage of vehicles with clean fuels as energy, and encourage travel by public transport are required to improve the particulate pollution originated from traffic emissions. The decrease trend of SO₂ in recent years indicates the improvement in coal combustion. However, low nitrogen combustion reform of key enterprises such as thermal power plants is required to further reduce nitrate generation.

5. Summary and Conclusions

The formation mechanisms of particulate pollution in Lanzhou remain unclear even though air pollution has been greatly improved in recent decades in Lanzhou. Multiple online data, including chemical species and PM concentrations with different sizes, gases, and meteorological factors at the LACMS station, were used to analyze the characteristics and reveal the formation mechanisms of particulate pollution during 2019–2020 winter in Lanzhou.

Average concentration of PM₁, PM_{2.5}, PM₁₀, and TSP in Lanzhou during the 2019–2020 winter was 45.7 ± 20.9, 70.4 ± 28.7, 114 ± 47.8, and 136.3 ± 60.9 μg m⁻³, respectively. The ratio of PM₁ to PM_{2.5} generally increased from 0.60 to 0.69 from low to high particulate pollution while the ratio of PM_{2.5} to PM₁₀ firstly increased with increasing particulate pollution and began to decrease under high PM conditions.

OM and SIAs were the major compositions of PM_{2.5} during 2019–2020 winter in Lanzhou. OM, nitrate, sulfate, and ammonium accounted for 35.8%, 16.6%, 12.7%, and 10.8%, respectively, of PM_{2.5} mass. The contribution of SIAs species decreased from low to high pollution level despite the increasing trend of SIAs concentrations with increasing PM_{2.5}. The contribution of SIAs was higher than carbonaceous species for the low pollution level while carbonaceous species became the major contributor for the high pollution level due to relative increase in carbonaceous species and decrease in SIAs.

The concentrations of nitrate and ammonium consistently increased with increasing PM_{2.5} while sulfate concentrations firstly increased but began to show little variation when PM_{2.5} went higher than 65 μg m⁻³. The SOR and NOR exhibited low values of 0.18 ± 0.12 and 0.11 ± 0.05, respectively. SOR exhibited decreasing trend under high PM_{2.5} conditions due to a decline in heterogeneous reactions and the reduced photochemical conversion of SO₂. NOR exhibited little dependence on RH because of limited aqueous phase generation of nitrate. NOR remained stagnant from low to high PM_{2.5} concentrations, which was a counteraction by opposite effects of decreasing O₃ and increasing ammonium. Results also show that ammonium rich samples dominated during 2019–2020 winter in Lanzhou. Diurnal variation of chemical species confirmed that SIAs were mainly originated from photochemical conversions rather than heterogeneous reactions.

The increasing nitrate to sulfate ratio and decreasing OC to EC ratio for high PM_{2.5} concentrations indicate relatively decreasing contribution of coal burning and increasing contribution of vehicle exhaust emissions on particulate pollution. The rapid decreasing trend of SOC to EC ratio under high PM concentrations was attributed to a combination of decreasing secondary photochemical conversions by reduced O₃ and the increasing accumulation of primary emissions by weakened atmospheric diffusion ability.

Despite the fact that particulate pollution in Lanzhou has been greatly improved in recent decades, our research suggests that the following issues should be carefully addressed to develop effective control measures: (1) The contribution of carbonaceous species (i.e., EC and OM) became higher than that of SIAs under high PM conditions; (2) the control measures failed to reduce the vehicle exhaust emissions in Lanzhou and led to evident increase of NO₂ in recent years; and (3) the influence of vehicle exhaust emissions on particulate pollution increased with the severity of particulate pollution.

Data Availability Statement

Online data of the LACMS station is available at the Semi-Arid Climate and Environment Observatory of Lanzhou University (SACOL; http://climate.lzu.edu.cn/English/Data_Sharing/LACMS_data.htm).

Acknowledgments

This research was supported by the National Natural Science Foundation of China (41905017), the Research on Causes of Air Pollution and Countermeasures in Area of Lanzhou Petrochemical Company (LZSH201924), and the Fundamental Research Funds for the Central Universities (lzujbky-2020-kb31 and lzujbky-2020-36). The authors thank the staffs from the Lanzhou Atmospheric Components Monitoring Superstation (LACMS) for the online gaseous and particulate pollution data.

References

An, X., Ma, A., & Liu, D. (2008). A GIS-based study for optimizing the Total emission control strategy in Lanzhou City. *Environmental Modeling and Assessment*, *13*(4), 491–501. <https://doi.org/10.1007/s10666-007-9096-4>

An, Z., Huang, R., Zhang, R., Tie, X., Li, G., Cao, J., et al. (2019). Severe haze in northern China: A synergy of anthropogenic emissions and atmospheric processes. *Proceedings of the National Academy of Sciences*, *116*(18), 8657–8666. <https://doi.org/10.1073/pnas.1900125116>

Brink, H., Otjes, R., & Weijers, E. (2019). Extreme levels and chemistry of PM from the consumer fireworks in the Netherlands. *Atmospheric Environment*, *212*, 36–40. <https://doi.org/10.1016/j.atmosenv.2019.04.046>

Cao, J., Lee, S. C., Chow, J. C., Watson, J. G., Ho, K. F., Zhang, R., et al. (2007). Spatial and seasonal distributions of carbonaceous aerosols over China. *Journal of Geophysical Research*, *112*, D22S11. <https://doi.org/10.1029/2006JD008205>

Cao, J., Tie, X., Dabberdt, W. F., Jie, T., Zhao, Z., An, Z., et al. (2013). On the potential high acid deposition in northeastern China. *Journal of Geophysical Research: Atmospheres*, *118*, 4834–4846. <https://doi.org/10.1002/jgrd.50381>

Castro, L. M., Pio, C. A., Harrison, R. M., & Smith, D. J. T. (1999). Carbonaceous aerosol in urban and rural European atmospheres: Estimation of secondary organic carbon concentrations. *Atmospheric Environment*, *33*(17), 2771–2781. [https://doi.org/10.1016/S1352-2310\(98\)00331-8](https://doi.org/10.1016/S1352-2310(98)00331-8)

Chen, C., Wang, H., Huang, J., Zhang, L., Qin, G., & Wang, J. (1993). Radiative effects of urban aerosols and implications for mixed layer development. *Chinese Science Bulletin*, *15*, 57–60. <https://doi.org/10.1360/csb1993-38-15-1399>

Chen, T., Chang, K., & Tsai, C. (2014). Modeling direct and indirect effect of long range transport on atmospheric PM_{2.5} levels. *Atmospheric Environment*, *89*, 1–9. <https://doi.org/10.1016/j.atmosenv.2014.01.065>

Chen, Y., Xie, S., Luo, B., & Zhai, C. (2017). Particulate pollution in urban Chongqing of southwest China: Historical trends of variation, chemical characteristics and source apportionment. *Science of the Total Environment*, *584*–585, 523–534. <https://doi.org/10.1016/j.scitotenv.2017.01.060>

Chow, J. C., Watson, J. G., Mauderly, J. L., Costa, D. L., Wyzga, R. E., Vedal, S., et al. (2006). Health effects of fine particulate air pollution: Lines that connect. *Journal of the Air & Waste Management Association*, *56*(6), 709–742. <https://doi.org/10.1080/10473289.2006.10464485>

Chu, P. C., Chen, Y., & Lu, S. (2008). Atmospheric effects on winter SO₂ pollution in Lanzhou, China. *Atmospheric Research*, *89*(4), 365–373. <https://doi.org/10.1016/j.atmosres.2008.03.008>

Chu, P. C., Chen, Y., Lu, S., Li, Z., & Lu, Y. (2008). Particulate air pollution in Lanzhou China. *Environment International*, *34*(5), 698–713. <https://doi.org/10.1016/j.envint.2007.12.013>

Ding, A., Huang, X., Nie, W., Sun, J., Kerminen, V. M., Petäjä, T., et al. (2016). Enhanced haze pollution by black carbon in megacities in China. *Geophysical Research Letters*, *43*, 2873–2879. <https://doi.org/10.1002/2016GL067745>

Dockery, D. W., & Pope, C. A. (1994). Acute respiratory effects of particulate air pollution. *Annual Review of Public Health*, *15*(1), 107–132. <https://doi.org/10.1146/annurev.pu.15.050194.000543>

Elser, M., Huang, R., Wolf, R., Slowik, J. G., Wang, Q., Canonaco, F., et al. (2016). New insights into PM_{2.5} chemical composition and sources in two major cities in China during extreme haze events using aerosol mass spectrometry. *Atmospheric Chemistry and Physics*, *16*(5), 3207–3225. <https://doi.org/10.5194/acp-16-3207-2016>

Feng, X., & Wang, S. (2012). Influence of different weather events on concentrations of particulate matter with different sizes in Lanzhou, China. *Journal of Environmental Sciences*, *24*(4), 665–674. [https://doi.org/10.1016/S1001-0742\(11\)60807-3](https://doi.org/10.1016/S1001-0742(11)60807-3)

Fu, Q., Zhuang, G., Wang, J., Xu, C., Huang, K., Li, J., et al. (2008). Mechanism of formation of the heaviest pollution episode ever recorded in the Yangtze River Delta, China. *Atmospheric Environment*, *42*(9), 2023–2036. <https://doi.org/10.1016/j.atmosenv.2007.12.002>

Fuzzi, S., Baltensperger, U., Carslaw, K., Decesari, S., Denier van der Gon, H., Facchini, M. C., et al. (2015). Particulate matter, air quality and climate: Lessons learned and future needs. *Atmospheric Chemistry and Physics*, *15*(14), 8217–8299. <https://doi.org/10.5194/acp-15-8217-2015>

Gartrell, G., & Friedlander, S. K. (1975). Relating particulate pollution to sources: The 1972 California aerosol characterization study. *Atmospheric Environment* (1967), *9*(3), 279–299. [https://doi.org/10.1016/0004-6981\(75\)90140-7](https://doi.org/10.1016/0004-6981(75)90140-7)

Guo, W., Zhang, Z., Zheng, N., Luo, L., Xiao, H., & Xiao, H. (2020). Chemical characterization and source analysis of water-soluble inorganic ions in PM_{2.5} from a plateau city of Kunming at different seasons. *Atmospheric Research*, *234*, 104687. <https://doi.org/10.1016/j.atmosres.2019.104687>

Hsu, S. C., Liu, S. C., Tsai, F., Engling, G., Lin, I. I., Chou, C. K. C., et al. (2010). High wintertime particulate matter pollution over an offshore island (Kinmen) off southeastern China: An overview. *Journal of Geophysical Research*, *115*(D17). <https://doi.org/10.1029/2009jd013641>

Huang, R., Zhang, Y., Bozzetti, C., Ho, K., Cao, J., Han, Y., et al. (2014). High secondary aerosol contribution to particulate pollution during haze events in China. *Nature*, *514*(7521), 218–222. <https://doi.org/10.1038/nature13774>

Huang, X., Ding, A., Wang, Z., Ding, K., Gao, J., Chai, F., & Fu, C. (2020). Amplified transboundary transport of haze by aerosol–boundary layer interaction in China. *Nature Geoscience*, *13*(6), 428–434. <https://doi.org/10.1038/s41561-020-0583-4>

Jiang, F., Liu, F., Lin, Q., Fu, Y., Yang, Y., Peng, L., et al. (2019). Characteristics and formation mechanisms of sulfate and nitrate in size-segregated atmospheric particles from urban Guangzhou, China. *Aerosol and Air Quality Research*, *19*(6), 1284–1293. <https://doi.org/10.4209/aaqr.2018.07.0251>

Kato, N. (1996). Analysis of structure of energy consumption and dynamics of emission of atmospheric species related to the global environmental change (SO_x, NO_x, and CO₂) in Asia. *Atmospheric Environment*, *30*(5), 757–785. [https://doi.org/10.1016/1352-2310\(95\)00110-7](https://doi.org/10.1016/1352-2310(95)00110-7)

Lanzhou Bureau of Statistics and Lanzhou Investigation team of National Bureau of Statistics (2020). Statistical Bulletin of National Economic and Social Development of Lanzhou City 2019. <http://tjj.lanzhou.gov.cn/module/download/downfile.jsp?classid=0&filename=1ed8e515051543bcada2eb19bb715e86.pdf>

Lei, Y., Shen, Z., Tang, Z., Zhang, Q., Sun, J., Ma, Y., et al. (2020). Aerosols chemical composition, light extinction, and source apportionment near a desert margin city, Yulin, China. *PeerJ*, *8*, e8447. <https://doi.org/10.7717/peerj.8447>

- Li, H., Ma, Y., Duan, F., He, K., Zhu, L., Huang, T., et al. (2017). Typical winter haze pollution in Zibo, an industrial city in China: Characteristics, secondary formation, and regional contribution. *Environmental Pollution*, 229, 339–349. <https://doi.org/10.1016/j.envpol.2017.05.081>
- Li, K., Jacob, D. J., Liao, H., Zhu, J., Shah, V., Shen, L., et al. (2019). A two-pollutant strategy for improving ozone and particulate air quality in China. *Nature Geoscience*, 12(11), 906–910. <https://doi.org/10.1038/s41561-019-0464-x>
- Li, M., Wang, T., Xie, M., Li, S., Zhuang, B., Huang, X., et al. (2019). Formation and evolution mechanisms for two extreme haze episodes in the Yangtze River Delta region of China during winter 2016. *Journal of Geophysical Research: Atmospheres*, 124, 3607–3623. <https://doi.org/10.1029/2019JD030535>
- Li, Z., Lau, W. K. M., Ramanathan, V., Wu, G., Ding, Y., Manoj, M. G., et al. (2016). Aerosol and monsoon climate interactions over Asia. *Reviews of Geophysics*, 54, 866–929. <https://doi.org/10.1002/2015RG000500>
- Liu, F., Tan, Q., Jiang, X., Yang, F., & Jiang, W. (2019). Effects of relative humidity and PM_{2.5} chemical compositions on visibility impairment in Chengdu, China. *Journal of Environmental Sciences*, 86, 15–23. <https://doi.org/10.1016/j.jes.2019.05.004>
- Liu, J., Fan, S., Zhang, L., Chen, C., Chen, X., & Meng, Z. (2006). Analysis on the pollution characteristics of atmospheric particle in Lanzhou City in winter. *Journal of Lanzhou University (Natural Sciences)*, 42(6), 45–49. <https://doi.org/10.13885/j.issn.0455-2059.2006.06.009>
- Makkonen, U., Virkkula, A., Mäntykenttä, J., Hakola, H., Keronen, P., Vakkari, V., & Aalto, P. P. (2012). Semi-continuous gas and inorganic aerosol measurements at a Finnish urban site: Comparisons with filters, nitrogen in aerosol and gas phases, and aerosol acidity. *Atmospheric Chemistry and Physics*, 12(12), 5617–5631. <https://doi.org/10.5194/acp-12-5617-2012>
- Ohta, S., & Okita, T. (1990). A chemical characterization of atmospheric aerosol in Sapporo. *Atmospheric Environment*, 24(4), 815–822. [https://doi.org/10.1016/0960-1686\(90\)90282-R](https://doi.org/10.1016/0960-1686(90)90282-R)
- Pathak, R. K., Wu, W. S., & Wang, T. (2009). Summertime PM_{2.5} ionic species in four major cities of China: nitrate formation in an ammonia-deficient atmosphere. *Atmospheric Chemistry and Physics*, 9(5), 1711–1722. <https://doi.org/10.5194/acp-9-1711-2009>
- Pye, H. O. T., Zuend, A., Fry, J. L., Isaacman-VanWertz, G., Capps, S. L., Appel, K. W., et al. (2018). Coupling of organic and inorganic aerosol systems and the effect on gas–particle partitioning in the southeastern US. *Atmospheric Chemistry and Physics*, 18(1), 357–370. <https://doi.org/10.5194/acp-18-357-2018>
- Qiu, X., Duan, L., Gao, J., Wang, S., Chai, F., Hu, J., et al. (2016). Chemical composition and source apportionment of PM₁₀ and PM_{2.5} in different functional areas of Lanzhou, China. *Journal of Environmental Sciences*, 40, 75–83. <https://doi.org/10.1016/j.jes.2015.10.021>
- Qu, W., Wang, Y., Wang, D., & Sheng, L. (2009). A review on the uncertainty in carbonaceous aerosol observation and investigation. *Climatic and Environmental Research (in Chinese)*, 14(2), 201–217. <https://doi.org/10.3878/j.issn.1006-9585.2009.02.10>
- Quan, J., Tie, X., Zhang, Q., Liu, Q., Li, X., Gao, Y., & Zhao, D. (2014). Characteristics of heavy aerosol pollution during the 2012–2013 winter in Beijing, China. *Atmospheric Environment*, 88, 83–89. <https://doi.org/10.1016/j.atmosenv.2014.01.058>
- Quirin, S. (2020). Why pollution is plummeting in some cities—But not others. *Nature*, 580(7803).
- Roig Rodelas, R., Perdrix, E., Herbin, B., & Riffault, V. (2019). Characterization and variability of inorganic aerosols and their gaseous precursors at a suburban site in northern France over one year (2015–2016). *Atmospheric Environment*, 200, 142–157. <https://doi.org/10.1016/j.atmosenv.2018.11.041>
- Rumsey, I. C., Cowen, K. A., Walker, J. T., Kelly, T. J., Hanft, E. A., Mishoe, K., et al. (2014). An assessment of the performance of the Monitor for Aerosols and Gases in ambient air (MARGA): A semi-continuous method for soluble compounds. *Atmospheric Chemistry and Physics*, 14(11), 5639–5658. <https://doi.org/10.5194/acp-14-5639-2014>
- Salako, G. O., Hopke, P. K., Cohen, D. D., Begum, B. A., Biswas, S. K., Pandit, G. G., et al. (2012). Exploring the variation between EC and BC in a variety of locations. *Aerosol and Air Quality Research*, 12(1), 1–7. <https://doi.org/10.4209/aaq.2011.09.0150>
- Shao, P., Tian, H., Sun, Y., Liu, H., Wu, B., Liu, S., et al. (2018). Characterizing remarkable changes of severe haze events and chemical compositions in multi-size airborne particles (PM₁, PM_{2.5} and PM₁₀) from January 2013 to 2016–2017 winter in Beijing, China. *Atmospheric Environment*, 189, 133–144. <https://doi.org/10.1016/j.atmosenv.2018.06.038>
- Shi, G., Xu, J., Shi, X., Liu, B., Bi, X., Xiao, Z., et al. (2019). Aerosol pH dynamics during haze periods in an urban environment in China: Use of detailed, hourly, speciated observations to study the role of ammonia availability and secondary aerosol formation and urban environment. *Journal of Geophysical Research: Atmospheres*, 124, 9730–9742. <https://doi.org/10.1029/2018JD029976>
- Stieger, B., Spindler, G., Fahlbusch, B., Müller, K., Grüner, A., Poulain, L., et al. (2018). Measurements of PM₁₀ ions and trace gases with the online system MARGA at the research station Melpitz in Germany—A five-year study. *Journal of Atmospheric Chemistry*, 75(1), 33–70. <https://doi.org/10.1007/s10874-017-9361-0>
- Sun, Y., He, Y., Kuang, Y., Xu, W., Song, S., Ma, N., et al. (2020). Chemical differences between PM₁ and PM_{2.5} in highly polluted environment and implications in air pollution studies. *Geophysical Research Letters*, 47, e2019GL086288. <https://doi.org/10.1029/2019GL086288>
- Sun, Y., Jiang, Q., Wang, Z., Fu, P., Li, J., Yang, T., & Yin, Y. (2014). Investigation of the sources and evolution processes of severe haze pollution in Beijing in January 2013. *Journal of Geophysical Research: Atmospheres*, 119, 4380–4398. <https://doi.org/10.1002/2014JD021641>
- Tan, J., Zhang, L., Zhou, X., Duan, J., Li, Y., Hu, J., & He, K. (2017). Chemical characteristics and source apportionment of PM_{2.5} in Lanzhou, China. *Science of the Total Environment*, 601–602, 1743–1752. <https://doi.org/10.1016/j.scitotenv.2017.06.050>
- Tang, X., & Li, J. (1989). Photochemical pollution in Lanzhou, China—A case study. *Journal of Environmental Sciences*, 01, 31–37. <https://doi.org/10.1007/s11434-012-5404-8>
- The State Council of the People's Republic of China (2013). Air pollution prevention and control action plan. http://www.gov.cn/zwqk/2013-09/12/content_2486773.htm
- Thishan Dharshana, K. G., Kravtsov, S., & Kahl, J. D. W. (2010). Relationship between synoptic weather disturbances and particulate matter air pollution over the United States. *Journal of Geophysical Research*, 115, D24219. <https://doi.org/10.1029/2010JD014852>
- Tian, D., Fan, J., Jin, H., Mao, H., Geng, D., Hou, S., et al. (2020). Characteristic and spatiotemporal variation of air pollution in Northern China based on correlation analysis and clustering analysis of five air pollutants. *Journal of Geophysical Research: Atmospheres*, 125, e2019JD031931. <https://doi.org/10.1029/2019JD031931>
- Tian, M., Liu, Y., Yang, F., Zhang, L., Peng, C., Chen, Y., et al. (2019). Increasing importance of nitrate formation for heavy aerosol pollution in two megacities in Sichuan Basin, southwest China. *Environmental Pollution*, 250, 898–905. <https://doi.org/10.1016/j.envpol.2019.04.098>
- Turpin, B. J., & Huntzicker, J. J. (1991). Secondary formation of organic aerosol in the Los Angeles basin: A descriptive analysis of organic and elemental carbon concentrations. *Atmospheric Environment Part A*, 25(2), 207–215. [https://doi.org/10.1016/0960-1686\(91\)90291-E](https://doi.org/10.1016/0960-1686(91)90291-E)

- Twigg, M. M., Di Marco, C. F., Leeson, S., van Dijk, N., Jones, M. R., Leith, I. D., et al. (2015). Water soluble aerosols and gases at a UK background site—Part 1: Controls of PM_{2.5} and PM₁₀ aerosol composition. *Atmospheric Chemistry and Physics*, *15*(14), 8131–8145. <https://doi.org/10.5194/acp-15-8131-2015>
- Venecek, M. A., Yu, X., & Kleeman, M. J. (2019). Predicted ultrafine particulate matter source contribution across the continental United States during summertime air pollution events. *Atmospheric Chemistry and Physics*, *19*(14), 9399–9412. <https://doi.org/10.5194/acp-19-9399-2019>
- Wang, G., Zhang, R., Gomez, M. E., Yang, L., Levy Zamora, M., Hu, M., et al. (2016). Persistent sulfate formation from London Fog to Chinese haze. *Proceedings of the National Academy of Sciences*, *113*(48), 13,630–13,635. <https://doi.org/10.1073/pnas.1616540113>
- Wang, H., Wang, Q., Gao, Y., Zhou, M., Jing, S., Qiao, L., et al. (2020). Estimation of secondary organic aerosol formation during a photochemical smog episode in Shanghai, China. *Journal of Geophysical Research: Atmospheres*, *125*, e2019JD032033. <https://doi.org/10.1029/2019JD032033>
- Wang, J., Li, X., Zhang, W., Jiang, N., Zhang, R., & Tang, X. (2016). Secondary PM_{2.5} in Zhengzhou, China: Chemical species based on three years of observations. *Aerosol and Air Quality Research*, *16*(1), 91–104. <https://doi.org/10.4209/aaqr.2015.01.0007>
- Wang, S., Feng, X., Zeng, X., Ma, Y., & Shang, K. (2009). A study on variations of concentrations of particulate matter with different sizes in Lanzhou, China. *Atmospheric Environment*, *43*(17), 2823–2828. <https://doi.org/10.1016/j.atmosenv.2009.02.021>
- Wang, Y., Gao, W., Wang, S., Song, T., Gong, Z., Ji, D., et al. (2020). Contrasting trends of PM_{2.5} and surface-ozone concentrations in China from 2013 to 2017. *National Science Review*, *7*(8), 1331–1339. <https://doi.org/10.1093/nsr/nwaa032>
- Wang, Y., Jia, C., Tao, J., Zhang, L., Liang, X., Ma, J., et al. (2016). Chemical characterization and source apportionment of PM_{2.5} in a semi-arid and petrochemical-industrialized city, Northwest China. *Science of the Total Environment*, *573*, 1031–1040. <https://doi.org/10.1016/j.scitotenv.2016.08.179>
- Wang, Y., Song, W., Yang, W., Sun, X., Tong, Y., Wang, X., et al. (2019). Influences of atmospheric pollution on the contributions of major oxidation pathways to PM_{2.5} nitrate formation in Beijing. *Journal of Geophysical Research: Atmospheres*, *124*, 4174–4185. <https://doi.org/10.1029/2019JD030284>
- Wang, Y., Zhang, Q., Jiang, J., Zhou, W., Wang, B., He, K., et al. (2014). Enhanced sulfate formation during China's severe winter haze episode in January 2013 missing from current models. *Journal of Geophysical Research: Atmospheres*, *119*, 10,425–10,440. <https://doi.org/10.1002/2013JD021426>
- Wang, Y., Zhang, X., Sun, J., Zhang, X., Che, H., & Li, Y. (2015). Spatial and temporal variations of the concentrations of PM₁₀, PM_{2.5} and PM₁ in China. *Atmospheric Chemistry and Physics*, *15*(23), 13,585–13,598. <https://doi.org/10.5194/acp-15-13585-2015>
- Wang, Y., Zhuang, G., Zhang, X., Huang, K., Xu, C., Tang, A., et al. (2006). The ion chemistry, seasonal cycle, and sources of PM_{2.5} and TSP aerosol in Shanghai. *Atmospheric Environment*, *40*(16), 2935–2952. <https://doi.org/10.1016/j.atmosenv.2005.12.051>
- Watson, J. G., Chow, J. C., & Houck, J. E. (2001). PM_{2.5} chemical source profiles for vehicle exhaust, vegetative burning, geological material, and coal burning in Northwestern Colorado during 1995. *Chemosphere*, *43*(8), 1141–1151. [https://doi.org/10.1016/S0045-6535\(00\)00171-5](https://doi.org/10.1016/S0045-6535(00)00171-5)
- Xiao, H., Zhu, R., Pan, Y., Guo, W., Zheng, N., Liu, Y., et al. (2020). Differentiation between nitrate aerosol formation pathways in a southeast Chinese city by dual isotope and modeling studies. *Journal of Geophysical Research: Atmospheres*, *125*, e2020JD032604. <https://doi.org/10.1029/2020JD032604>
- Xie, Y., Liu, Z., Wen, T., Huang, X., Liu, J., Tang, G., et al. (2019). Characteristics of chemical composition and seasonal variations of PM_{2.5} in Shijiazhuang, China: Impact of primary emissions and secondary formation. *Science of the Total Environment*, *677*, 215–229. <https://doi.org/10.1016/j.scitotenv.2019.04.300>
- Xu, J., Shi, J., Zhang, Q., Ge, X., Canonaco, F., Prévôt, A. S. H., et al. (2016). Wintertime organic and inorganic aerosols in Lanzhou, China: Sources, processes, and comparison with the results during summer. *Atmospheric Chemistry and Physics*, *16*(23), 14,937–14,957. <https://doi.org/10.5194/acp-16-14937-2016>
- Yao, L., Garmash, O., Bianchi, F., Zheng, J., Yan, C., Kontkanen, J., et al. (2018). Atmospheric new particle formation from sulfuric acid and amines in a Chinese megacity. *Science*, *361*(6399), 278–281. <https://doi.org/10.1126/science.aao4839>
- Ye, S., Ma, T., Duan, F., Li, H., He, K., Xia, J., et al. (2019). Characteristics and formation mechanisms of winter haze in Changzhou, a highly polluted industrial city in the Yangtze River Delta, China. *Environmental Pollution*, *253*, 377–383. <https://doi.org/10.1016/j.envpol.2019.07.011>
- Zhang, J., Reid, J. S., Alfaro-Contreras, R., & Xian, P. (2017). Has China been exporting less particulate air pollution over the past decade? *Geophysical Research Letters*, *44*, 2941–2948. <https://doi.org/10.1002/2017GL072617>
- Zhang, L., & Chen, C. (1994). Research on air pollution and its control of Lanzhou area. *Journal of Lanzhou University (Natural Sciences)*, *(001)*, 137. <https://doi.org/10.13885/j.issn.0455-2059.1994.01.028>
- Zhang, L., Chen, C., & Murlis, J. (2001). Study on winter air pollution control in Lanzhou, China. *Water, Air, and Soil Pollution*, *127*(1/4), 351–372. <https://doi.org/10.1023/A:1005257722202>
- Zhang, W., Zhang, X., Zhong, J., Wang, Y., Wang, J., Zhao, Y., & Bu, S. (2019). The effects of the “two-way feedback mechanism” on the maintenance of persistent heavy aerosol pollution over areas with relatively light aerosol pollution in northwest China. *Science of the Total Environment*, *688*, 642–652. <https://doi.org/10.1016/j.scitotenv.2019.06.295>
- Zhang, Y., Tang, L., Croteau, P. L., Favez, O., Sun, Y., Canagaratna, M. R., et al. (2017). Field characterization of the PM_{2.5} Aerosol Chemical Speciation Monitor: Insights into the composition, sources, and processes of fine particles in eastern China. *Atmospheric Chemistry and Physics*, *17*(23), 14,501–14,517. <https://doi.org/10.5194/acp-17-14501-2017>
- Zheng, G., Duan, F., Su, H., Ma, Y., Cheng, Y., Zheng, B., et al. (2015). Exploring the severe winter haze in Beijing: The impact of synoptic weather, regional transport and heterogeneous reactions. *Atmospheric Chemistry and Physics*, *15*(6), 2969–2983. <https://doi.org/10.5194/acp-15-2969-2015>